

COMPARATIVE ANALYSIS OF THE FLOW IN THE BOILER DUST SYSTEMS WITH THE ELBOW

Jacek WYDRYCH¹, Bolesław DOBROWOLSKI²

^{1,2} *Opole University of Technology, Department of Thermal Engineering and Industrial Facilities, Mikołajczyka 5, 45-271 Opole, Poland*

E-mail: j.wydrych@po.opole.pl, b.dobrowolski@po.opole.pl

Abstract

In the case of designing and service of the pneumatic conveying systems for power boilers, presence of the solid particle segregation in some areas is an important problem. In many cases, in such systems diversification of concentration and out-of-control segregation of particles take place. In a consequence, diversification of propagation, disturbances of the combustion process and accelerated erosion of the installation elements can occur. Moreover in the large power boilers, the required separation of the air-dust mixture to particular burners has to be obtained. This problem is very important because of limitation of losses of incomplete combustion, life of many furnace elements and NO_x emission.

It is the outlet straight interval of the dust tube from the mill together with the elbow. The four-path separator is located just above the elbow. The tests of gas and dust separation show the problem of non-uniformity of their distribution. From the results it appears that particle distribution to particular outlets is non-uniform under different service conditions of the system.

In the paper was presented multi-phase models of flow in set with elbow. In work three methods Euler-Euler, Euler-Lagrange and E-L with modification was compared with results of experiments.

The Euler-Lagrange model is usually applied for tests of the multiphase gas-solid particle mixture motion. It provides good quality of the results for volume fractions of solid particles not exceeding 12%. From tests of elements as elbows, separators or cyclone separators it appears that in some of their areas the limit value 12% is exceeded. This work shows that the Euler-Euler model seems to be more useful for the considered flows.

Key words: CFD, pneumatic conveying systems

INTRODUCTION

In the case of designing and service of the pneumatic conveying systems for power boilers, presence of the solid particle segregation in some areas is an important problem. In many cases, in such systems diversification of concentration and out-of-control segregation of particles take place. In a consequence, diversification of propagation, disturbances of the combustion process and accelerated erosion of the installation elements can occur (Dobrowolski et al., 2006), (Lu et al., 2009), (Wydrych, 2007), (Wydrych, 2011). Moreover in the large power boilers, the required separation of the air-dust mixture to particular burners has to be obtained. This problem is very important because of limitation of losses of incomplete combustion, life of many furnace elements and NO_x emission.

The design problems connected with the pneumatic conveying systems are the subject of many research works (Akilli et al., 2001), (Miller et al., 2009), (Triesch et al 2001). In many papers we can find equations determining linear and local resistances of different elements of

the installation (El-Behery et al., 2009). They include, among others, influence of the dispersed phase, the substitute diameter of particles and spatial location of the elements on losses of pressure (Hidayat et al., 2005), (Lu et al., 2009). Much attention was paid to conditions under which the dust can accumulate in the installation (Dobrowolski et al., 2006), (Fokeer et al., 2004). This problem is very important because of the required mixture separation and work safety. Many papers are devoted to experimental and numerical investigations of the flow in the pneumatic conveying systems (Albion et al., 2007), (Borsuk et al., 2006), (Hidayat et al., 2005), (Levy et al., 1998), (Rajniak et al., 2008), (Woods et al., 2008). Many papers were devoted to different separators included into dust-pipe installations (Bilirgen et al., 2001), (Dobrowolski et al., 2004), (Laín et al., 2012). In the furnace installation in the Opole Power plant there are two-path separators with mobile baffles and four-path separators, allowing to control distribution. Such structures were subjected to numerical investigations, many measurements were done, too.

This paper presents numerical tests of the flow of the air-coal dust mixture through the pipeline with the build-up elbow. The tests were performed in order to qualitative and quantitative comparison of the calculation results for two methods of simulation: the Euler-Lagrange and the Euler-Euler methods. Strong diversification of concentration and particle segregation within the elbow caused diversification of concentration of the mixture silt to the four-path separator located directly above be the elbow (Spedding et al., 2007), (Wang et al., 2001). It was a reason of the diversified dust propagation after the separator and accelerated erosion of separators. Its influence on the particle separation was tested with two methods. The considered flow system is shown in Fig. 1.

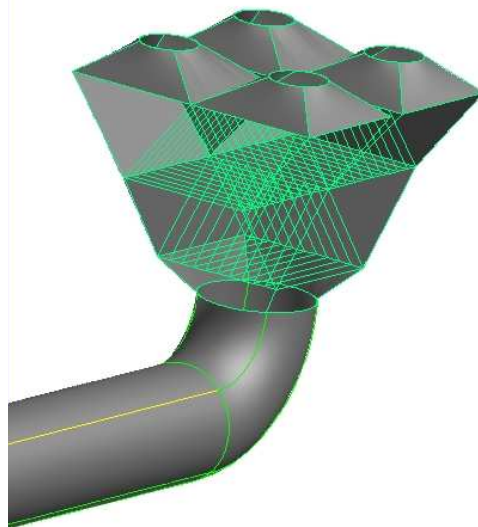


Fig. 1. General view of the examine four-path separator system

It is the outlet straight interval of the dust tube from the mill together with the elbow. The four-path separator is located just above the elbow. The tests of gas and dust separation show the problem of non-uniformity of their distribution. From the results it appears that particle distribution to particular outlets is non-uniform under different service conditions of the system.

The Euler-Lagrange model is usually applied for tests of the multiphase gas-solid particle mixture motion. It provides good quality of the results for volume fractions of solid particles not exceeding 12%. From tests of elements as elbows, separators or cyclone separators it appears that in some of their areas the limit value 12% is exceeded (Jaworski et al., 2002). This work shows that the Euler-Euler model seems to be more useful for the considered flows (Wydrych et al., 2010), (Wydrych, 2010).

SIMULATION OF MULTIPHASE FLOWS

Presence of the particles in the gas stream influences the gas motion, and this influence depends on the particle concentration. In the simplest case, the mixture motion can be described by introduction of the substitute density to the equations of motion. In simulation of motion of the diluted gas-particles mixture, two approaches are applied (Fokeer et al., 2004):

- particular particles are treated as the material points displacing in the space, and their interactions with gas and the walls are taken into account (the Lagrange method) (Laín et al., 2012),
- the particle phase is replaced by the fictitious fluid with suitably defined physical properties (the Euler method).

Simulation with the Euler-Lagrange method

In order to realize numerical tests, the mathematical model containing equations of motion for the gaseous phase and coal dust particles was applied. The air motion was described with the Euler method, and the particle motion – by the Lagrange method. It is possible to analyze motion of the gas-particle polydispersive mixture, in this paper the PSICell method was applied.

Simulation of the gaseous phase flow

Neglecting the phase changes and assuming that both phases are incompressible, and the flow is isothermal and stationary, the gas motion can be described in the uniform, generalized conservative form, isolating convection, diffusion and source components. In a consequence we obtain

$$\frac{\partial(\rho\phi)}{\partial t} + \frac{\partial(\rho U_i \phi)}{\partial x_i} = \frac{\partial}{\partial x_i} \left(\Gamma_\phi \frac{\partial \phi}{\partial x_i} \right) + S_\phi + S_{\phi p} \quad (1)$$

where ϕ is a generalized dependent variable, Γ_ϕ is the coefficient of diffusion transport, and the source term S_ϕ contains all the remaining components of the differential equations (except for convection and diffusion ones). The coefficients Γ_ϕ and S_ϕ are dependent on the variable ϕ . In the PSICell method it is assumed that particles of the disintegrated phase are the sources of mass, momentum and energy occurring as additional components $S_{\phi p}$ in equations of the continuous (gaseous) phase.

The system of equations is accompanied by suitable boundary and initial conditions. The above system of partial differential equations is non-linear. Particular equations are coupled, so they have to be solved with special numerical techniques.

In order to calculate turbulence model k- ϵ was used. The standard k- ϵ model is a semi-empirical model based on model transport equations for the turbulence kinetic energy k and its dissipation rate ϵ . The model transport equation for k is derived from the exact equation, while the model transport equation for ϵ was obtained using physical reasoning and bears little resemblance to its mathematically exact counterpart (Wang et al., 2001).

In the derivation of the k- ϵ model, it was assumed that the flow was fully turbulent, and the effects of molecular viscosity were negligible. The standard k- ϵ model is therefore valid only for fully turbulent flows (Akilli et al., 2001). The turbulence kinetic energy, k , and its rate of dissipation, ϵ , are obtained from the following transport equations (Kuan et al., 2007):

$$\frac{\partial}{\partial t} (\rho k) + \frac{\partial}{\partial x_i} (\rho k u_i) = \frac{\partial}{\partial x_j} \left[\left(\mu + \frac{\mu_t}{\sigma_k} \right) \frac{\partial k}{\partial x_j} \right] + G_k + G_b - \rho \epsilon - Y_M + S_k \quad (2)$$

$$\frac{\partial}{\partial t}(\rho\varepsilon) + \frac{\partial}{\partial x_i}(\rho\varepsilon u_i) = \frac{\partial}{\partial x_j} \left[\left(\mu + \frac{\mu_t}{\sigma_\varepsilon} \right) \frac{\partial \varepsilon}{\partial x_j} \right] + C_{1\varepsilon} \frac{\varepsilon}{k} (G_k + C_{3\varepsilon} G_b) - C_{2\varepsilon} \rho \frac{\varepsilon^2}{k} + S_\varepsilon \quad (3)$$

In these equations, G_k represents the generation of turbulence kinetic energy due to the mean velocity gradients. G_b is the generation of turbulence kinetic energy due to buoyancy. Y_M represents the contribution of the fluctuating dilatation in compressible turbulence to the overall dissipation rate. $C_{1\varepsilon}$, $C_{2\varepsilon}$, and $C_{3\varepsilon}$ are constants. σ_k and σ_ε are the turbulent Prandtl numbers for k and ε , respectively. S_k and S_ε are user-defined source terms. The turbulent (or eddy) viscosity μ_t is computed by combining k and ε as follows:

$$\mu_t = \rho C_\mu \frac{k^2}{\varepsilon} \quad (4)$$

The model constants $C_{1\varepsilon}$, $C_{2\varepsilon}$, C_μ , σ_k and σ_ε have the following default values $C_{1\varepsilon} = 1.44$, $C_{2\varepsilon} = 1.92$, $C_\mu = 0.09$, $\sigma_k = 1.0$ and $\sigma_\varepsilon = 1.3$.

These default values have been determined from experiments with air and water for fundamental turbulent shear flows including homogeneous shear flows and decaying isotropic grid turbulence. They have been found to work fairly well for a wide range of wall-bounded and free shear flows.

Simulation of the solid particle flow

The particle trajectory should be known during calculation of the mentioned above source components. The particle trajectory is calculated according to its equation of motion. If the phase density difference is big, the equation of particle motion can be written as (Laín et al., 2012):

$$m_p \frac{du_p}{dt} = \frac{3}{4} C_D \frac{\rho m_p}{\rho_p d_k} u |u - u_p| (u - u_p) + g \quad (5)$$

where m_p is mass of the particle, and C_D is the aerodynamic drag coefficient (Bilirgen et al., 2001). Special attention should be paid to the case when the particle collides with the wall. In such a case, components of the particle velocity vector after the collision are calculated from the following equations (Kuan et al., 2007):

$$u_{p1} = e_t u_p, \quad v_{p1} = -e_n v_p \quad (6)$$

where e_t and e_n define coefficients of restitution in shear and normal directions to the wall surface, u_p , v_p , are forward speeds in directions x , and y (Kosinski et al., 2010). In Eq.(6), the subscript 1 means a component of the particle velocity after collision (Triesch et al., 2001).

Dependences of the coefficient of restitution on the particle glancing angle for the given pairs of materials are obtained during tests. The dependences for the pair stainless steel 410 – quartz sand are expressed by the following equations :

$$\begin{aligned} e_t &= 0.988 - 1.66\alpha + 2.11\alpha^2 - 0.67\alpha^3 \\ e_n &= 0.993 - 1.76\alpha + 1.56\alpha^2 - 0.49\alpha^3 \end{aligned} \quad (7)$$

Turbulent dispersion of particles can be modeled using a stochastic discrete-particle approach. In the stochastic tracking approach, FLUENT predicts the turbulent dispersion of particles by integrating the trajectory equations for individual particles, using the instantaneous fluid velocity, $\bar{u} = u'(t)$, along the particle path during the integration (Levy et al., 1998). By computing the trajectory in this manner for a sufficient number of representative particles, the random effects of turbulence on the particle dispersion may be accounted for. In FLUENT, the Discrete Random Walk (DRW) model is used. In this model, the fluctuating velocity components are discrete piecewise constant functions of time. Their random value is kept constant over an interval of time given by the characteristic lifetime of

the eddies. The DRW model may give non-physical results in strongly inhomogeneous diffusion-dominated flows, where small particles should become uniformly distributed. Instead, the DRW will show a tendency for such particles to concentrate in low-turbulence regions of the flow (Yilmaz et al., 2001).

Moreover, for calculation the drag coefficient, C_D , can be used the shape factor ϕ , which is taken from Haider and Levenspiel model. The shape factor is defined as

$$\phi = \frac{s}{S} \quad (8)$$

where s is the surface area of a sphere having the same volume as the particle, and S is the actual surface area of the particle.

Simulation with the Euler-Euler method

Simulation of the flows in conveying systems requires including more than one phase in the flow (Wydrych et al., 2010). Presence of at least two phases in the mixture provides presence of different flow patterns depending on flow intensity of particular phases, their physical properties and the considered geometry.

In the case of pneumatic conveying, analysis was based on numerical solutions performed with the Euler method and the Fluent program (Wydrych et al., 2010). The Euler-Euler method was applied where the discrete phase was included as a substitute continuous medium penetrating the gaseous phase. Substitution of the diluted phase by the continuous medium causes that it is necessary to determine properties of this medium similarly like in the case of real continuous media. For such medium defined as granular, temperature, pressure and granular viscosity are calculated. Procedure of determination of these properties is presented in this paper.

General mass and momentum conservation laws are the same as equations for one-phase flows and they are also valid for multiphase flows. In order to include two or more phases in the control areas, a concentration measure of single phases in the mixture. This measure is the volume fraction which in the balanced volume is defined as:

$$\alpha_k = \frac{1}{V} \int_V X_k(r) dV \quad (9)$$

where $X_k(r)$ takes the value 1 or 0 depending on that if the differential volume dV of the coordinate r contains the phase „k” or not (Dodds et al., 2011). According to the rules of fraction summation after all the occurring phases “n”, the following equality is valid:

$$\sum_{k=1}^n \alpha_k = 1 \quad (10)$$

The efficient density of phase „k” is described by:

$$\rho_k = \alpha_k \rho_k \quad (11)$$

In the case of simulation of multiphase gas-solid flows while fluidization, the heterogeneous Euler-Euler model (the Euler model) is applied. In this model, separate equations are formulated for each phase, and in the control areas their averaged properties are taken into account. In the case of the Euler model, the equations of mass and momentum conservation are similar to the equations for the uniaxial model. In the assumed Euler method, the disintegrated material is included as the substitute granular continuous medium penetrating the gaseous phase. If there is no mass exchange between the considered phases, the equation of motion and continuity for phase “k” are (Hidayat et al., 2005):

$$\frac{\partial(\alpha_k \rho_k \bar{u}_k)}{\partial t} + \nabla \cdot (\alpha_k \rho_k \bar{u}_k \bar{u}_k) = -\alpha_k \nabla p + \nabla \cdot (\alpha_k T_k) + \alpha_k \rho_k \bar{g} + \alpha_k \rho_k (\bar{F}_k + \bar{F}_s) \quad (12)$$

$$\frac{\partial(\alpha_k \rho_k)}{\partial t} + \nabla \cdot (\alpha_k \rho_k \bar{u}_k) = 0. \quad (13)$$

The tensor T_k is described by :

$$T_k = \alpha_k \mu_k (\nabla \bar{u}_k + \nabla \bar{u}_k^T) + \alpha_k \left(\lambda_k - \frac{2}{3} \mu_k \right) \nabla \cdot \bar{u}_k I \quad (14)$$

The superscript T concerns transposition of the velocity gradient tensor. The vector \bar{F}_s including the forces generated by contacts of solid particles concerns only the balance of momentum for the disintegrated „granular” solid phase, and for fluids it is equal to zero. This component includes the results of interactions between particles, means solid phase viscosity, and shear stresses for the solid particle $2\mu_k S_k$. Similarly like in the case of fluids, the granular absolute viscosity μ_k and volumetric viscosity λ_k are included. A value of the vector \bar{F}_s for the disintegrated solid phase, understood as a semi-continuous fluid is calculated in a similar way as for influence of the stresses occurring in liquid phases, i.e. from (Hidayat et al., 2005):

$$\bar{F}_s = \nabla \cdot (2\mu_k S_k - p_k I) \quad (15)$$

The momentum exchange between phases is influenced by force of gravity and force of aerodynamic drag. Interfacial action \bar{F}_k can be described by the following expression:

$$\bar{F}_k = K_k (\bar{u} - \bar{u}_k) \quad (16)$$

The coefficient K_k can be written in the following general form:

$$K_k = \frac{\alpha_k \rho_k f}{\tau_d} \quad (17)$$

Time of dynamic relaxation of the particle can be written as:

$$\tau_d = \frac{\rho_k d_k^2}{18\mu} \quad (18)$$

The coefficient of interfacial momentum exchange K_k in the Gidaspow model, assumed while tests, can be written as (Wydrych et al., 2010):

- for a volume fraction of the continuous phase $\alpha > 0,8$

$$K_k = \frac{3}{4} C_D \frac{\alpha_k \alpha \rho |\bar{u}_k - \bar{u}|}{d_k} \alpha^{-2,65} \quad (19)$$

where coefficient C_D is expressed by the relationship (Spedding et al., 2007):

$$C_D = \frac{24}{\alpha \text{Re}_k} \left[1 + 0,15 (\alpha \text{Re}_k)^{0,687} \right] \quad (20)$$

- for a volume fraction of the continuous phase $\alpha \leq 0,8$

$$K_k = 150 \frac{\alpha_k (1 - \alpha) \mu}{\alpha d_k^2} + 1,75 \frac{\rho \alpha_k |\bar{u}_k - \bar{u}|}{d_k} \quad (21)$$

The Reynolds number is expressed as

$$\text{Re} = \frac{\rho d_k |\bar{u}_k - \bar{u}|}{\mu} \quad (22)$$

In multiphase flows of disintegrated particles, granular pressures are determined independently for each disintegrated phase. Next they are applied for determination of the pressure gradient in the equations of motion. In order to determine granular pressures and granular viscosities it is necessary to introduce granular temperatures into the model. Granular pressure can be expressed as:

$$p_k = \alpha_k \rho_k \Theta_k + 2\rho_k (1 + e_{kk}) \alpha_k^2 g_{0kk} \Theta_k \quad (23)$$

Coefficient g_{0kk} can be described by :

$$g_{0kk} = \left[1 - \left(\frac{\alpha_k}{\alpha_{k,\max}} \right)^{\frac{1}{3}} \right]^{-1} \quad (24)$$

Granular temperature is proportional to kinetic energy of fluctuation of solid particle motion and the equation of transport coming from the kinetic theory where granular temperature of phase „k” is proportional to kinetic energy of the random motion of particles can be expressed as:

$$\frac{3}{2} \left[\frac{\partial}{\partial t} (\rho_k \alpha_k \Theta_k) + \nabla \cdot (\rho_k \alpha_k \bar{u}_k \Theta_k) \right] = (-p_k I + T_k) : \nabla \bar{u}_k + \nabla \cdot (k_{\Theta_k} \nabla \Theta_k) - \gamma_{\Theta_k} + \phi_k \quad (25)$$

where $(-p_k I + T_k) : \nabla \bar{u}_k$ is energy generated by the stress tensor for the solid particle, $(k_{\Theta_k} \nabla \Theta_k)$ is energy diffusion and the diffusion coefficient k_{Θ_k} is dependent on granular temperature and it is expressed as:

$$k_{\Theta_k} = \frac{150 \rho_k d_k \sqrt{(\Theta_k \pi)}}{384 (1 + e_{kk}) g_{0kk}} \left[1 + \frac{6}{5} \alpha_k g_{0kk} (1 + e_{kk}) \right]^2 + 2 \rho_k \alpha_k^2 d_k (1 + e_{kk}) g_{0kk} \sqrt{\frac{\Theta_k}{\pi}} \quad (26)$$

The coefficient of energy dissipation while particle collisions is expressed by:

$$\gamma_{\Theta_k} = \frac{12(1 - e_{kk}^2) g_{0kk}}{d_k \sqrt{\pi}} \rho_k \alpha_k^2 \Theta_k^{3/2} \quad (27)$$

Energy transfer during random fluctuations of velocities of particles of phase „k” to the gas or other disintegrated phases can be written in the following form:

$$\phi_k = -3K_k \Theta_k \quad (28)$$

Neglecting convection and diffusion, it is possible to use the algebraic relationship for determination of granular temperature.

In equations of motion of the phase „k” there is the coefficient of volume viscosity λ_k , including resistance of the disintegrated phase against compression and expansion, which is determined from:

$$\lambda_k = \frac{4}{3} \alpha_k \rho_k d_k g_{0kk} (1 + e_{kk}) \left(\frac{\Theta_k}{\pi} \right)^{1/2} \quad (29)$$

The coefficient of absolute viscosity μ_k , calculated from:

$$\mu_k = \mu_{k,col} + \mu_{k,kin} + \mu_{k,fr} \quad (30)$$

where the components are collision, kinetic and friction viscosities (Triesch et al., 2001). Particular components are calculated from

$$\mu_{k,col} = \frac{4}{5} \alpha_k \rho_k d_k g_{0kk} (1 + e_{kk}) \left(\frac{\Theta_k}{\pi} \right)^{1/2} \quad (31)$$

$$\mu_{k,kin} = \frac{10 \rho_k d_k \sqrt{\Theta_k \pi}}{96 \alpha_k (1 + e_{kk}) g_{0kk}} \left[1 + \frac{4}{5} g_{0kk} \alpha_k (1 + e_{kk}) \right]^2 \quad (32)$$

$$\mu_{k,fr} = \frac{p_k \sin \phi}{2 \sqrt{I_{2D}}} \quad (33)$$

The Euler model is the most complex model accessible in the package FLUENT. While realization of calculations the equations of motion and continuity are solved for each phase. Coupling between them is realized by pressure and coefficients of interphase exchanges. In the case of granular flows applied while calculations for pneumatic conveying, the properties characterizing the flow are obtained by application of kinetic theory. In the case of multiphase flow realized with the Euler method, the solution is based on the following assumptions (Wydrych et al., 2010):

- in the control area for all the phases the same pressure is valid,
- the equations of continuity and motion are formulated for each phase,
- in the case of the disintegrated phase the following parameters are introduced:
 - granular temperature calculated for each disintegrated phase with use of algebraic relationships,
 - coefficients of granular absolute and volume viscosities obtained with kinetic theory similar to kinetic theory for gases.

THE RESULTS OF NUMERICAL SIMULATION

An attempt of qualitative and quantitative assessment of the simulation results obtained with two methods was performed for flow system of the inlet interval before the separator. In order to make calculations the continuous flow systems were replaced by the calculation areas including non-structural calculation networks. The network includes 372846 calculation elements of volumes $5.59 \cdot 10^{-6} \div 1.88 \cdot 10^{-4} \text{ m}^3$. Fig. 1 shows the tested systems, i.e. the elbow located before the four-path separator. The figure presents discretization of the tested areas to the calculation networks.

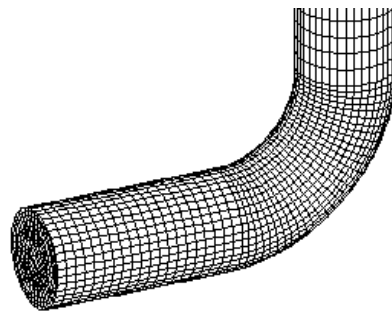


Fig. 2. Discretization of the calculation area

The FLUENT program was applied for numerical calculations. It allows to solve the systems of equations of mass transport, gas momentum and the solid phase completed with the turbulence model equations. Calculations were made according to the Euler-Lagrange method (the **EL** method) and the Euler-Euler method (the **EE** method). Moreover calculations

were made with use Euler-Lagrange method completed by particle turbulence effect and particle shape effect (the **ELpl** method).

Disintegrated coal particles for diameters d_k : 15, 90, 125, 200 μ m were tested. Calculations were realized for a stationary flow with interfacial coupling, and at the inlet to the calculation area stationary velocity distributions of the gaseous phase were assumed. The inlet velocity was at level 30m/s. The presented results concern only the inlet to the system together with the tested elbow, and the separator was not taken into account.

Fig.3 presents distributions of the gas velocity modulus and pressure obtained with the EE method – a), b), the EL method – c), d) and the ELpl method – e), f). Analysis of velocity distributions in the tested system gives information about positions of zones of the increased and decreased velocities. The velocity increase takes place along the internal sides of the elbows. The decreased velocity zone can cause accumulation of solid particles in its volume.

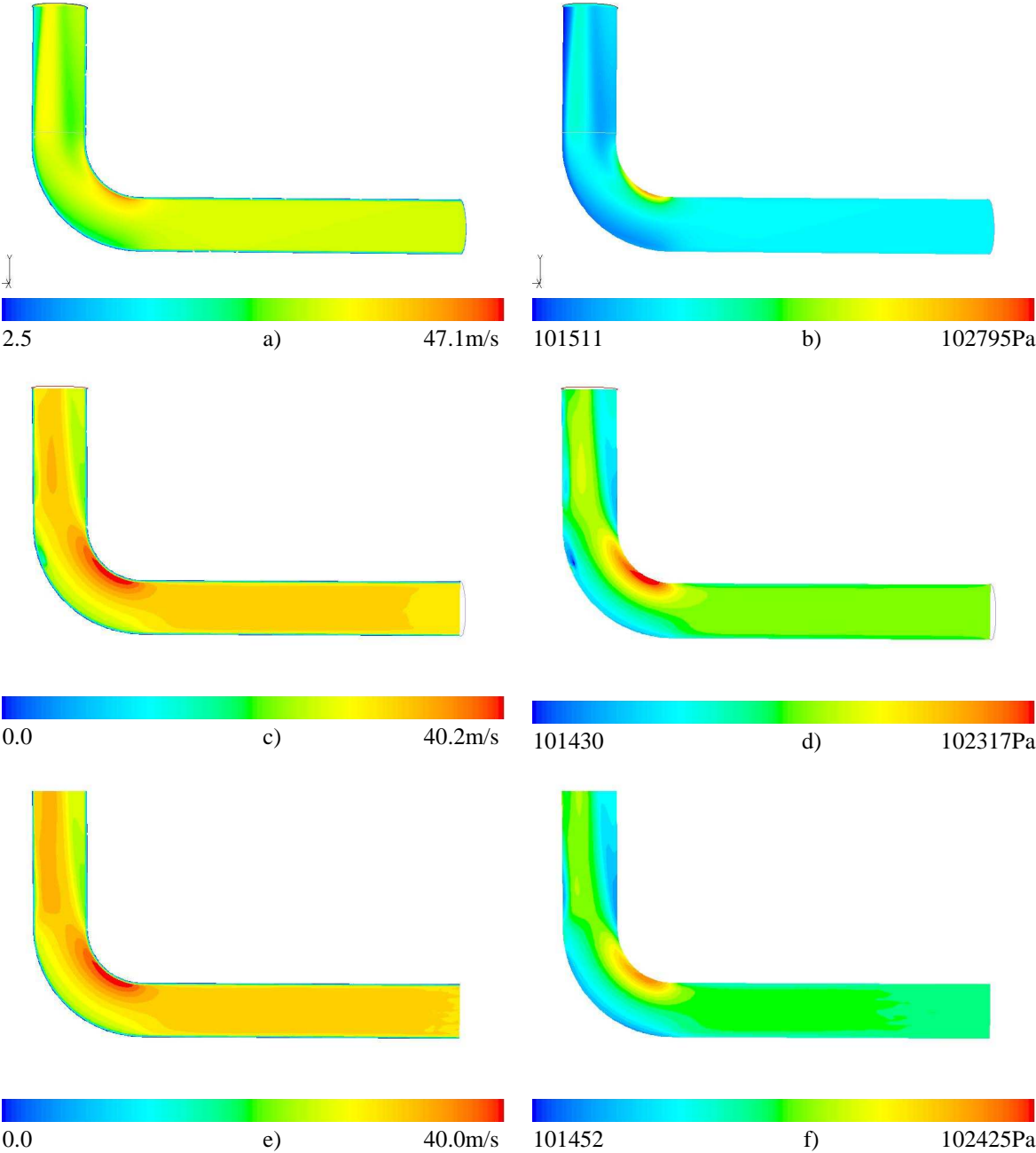
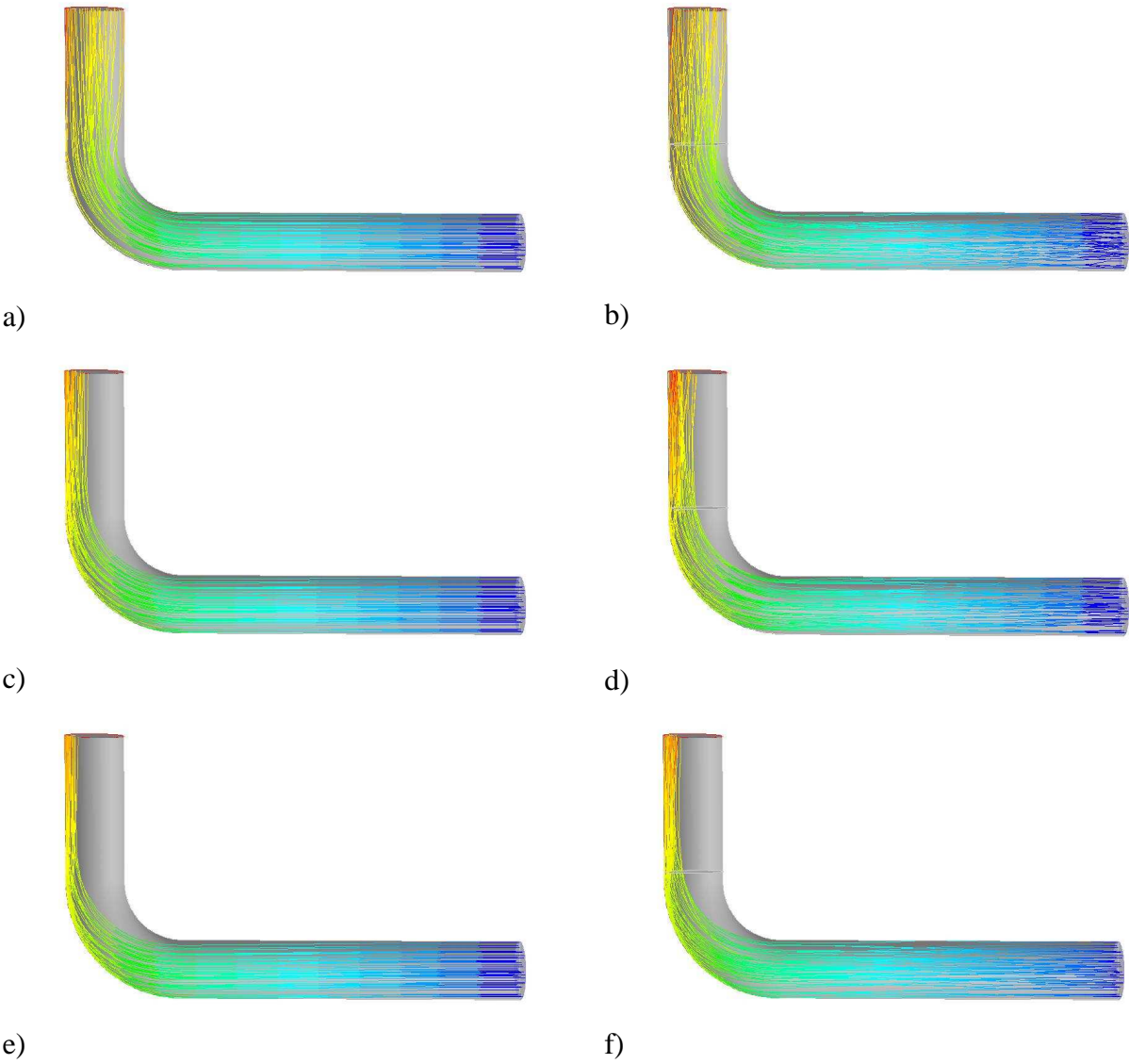


Fig. 3. The velocity and pressure fields obtained with the methods a), b) – EE, c), d) – EL and e), f) – ELpl

In the case of the Euler-Lagrange model, when convergence of the velocity field solution is obtained and presence of solid particles and coupling between the phases are taken into account, trajectories of motion of the coal dust particles of density 1300kg/m^3 are calculated. Fig.4 shows the results of calculations of trajectories of the particles delivered to the system from the point inlets for the inlet velocity 30m/s obtained with the EL method – a), c), e), g) and the ELpl method – b), d), f), h). Different colours mark the particle residential time, for which maximum value is in a range $0.546\div 0.556\text{s}$. The figure presents the trajectories of the particles $15, 90, 125$ and $200\mu\text{m}$ in diameters under vertical distribution of the point inlets of the supplying section.



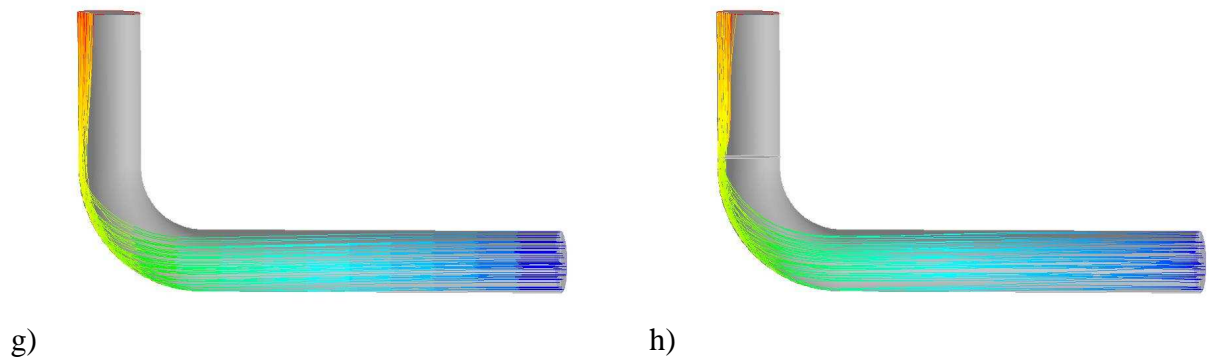
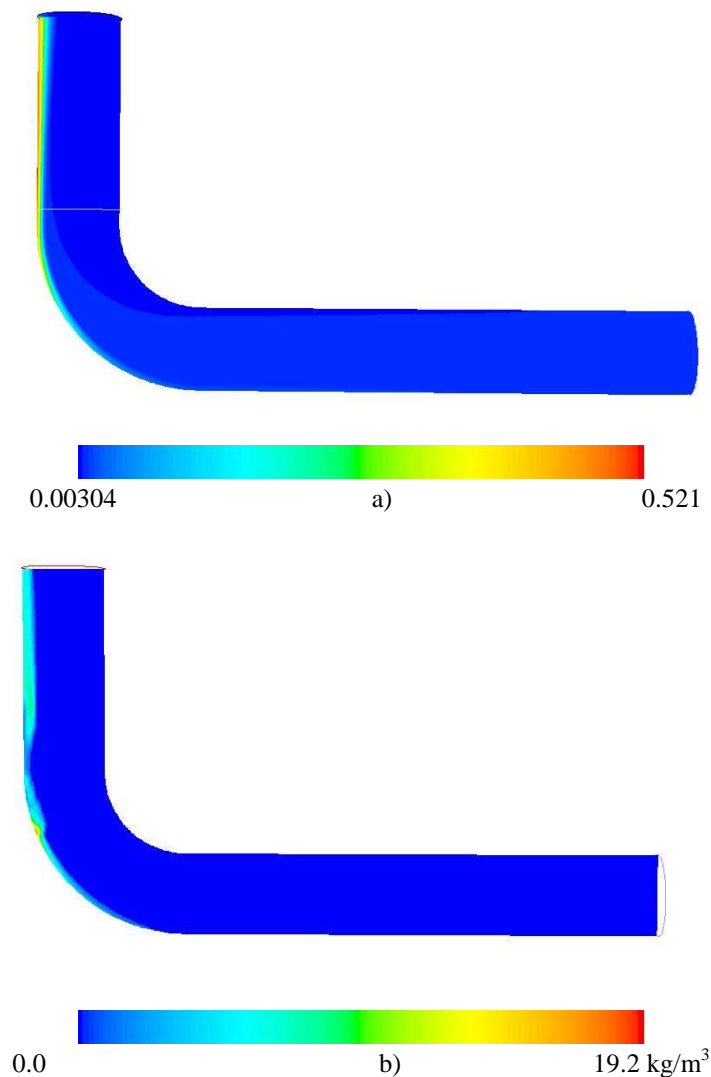


Fig. 4. Trajectories of the particles obtained with the methods a), c), e), g) – EL, and b), d), f), h) – EL for particles a), b) - 15µm, c), d) - 90µm, e), f) - 125µm and g), h) - 200µm

From analysis of the trajectories it appears that the particles of small diameters move along the paths corresponding to lines of the gaseous phase current, and the particles of big diameters often move along to the paths forming a “cord”, this is a reason of local increase of concentration (Bilirgen et al., 2001), (Borsuk et al., 2006), (Fokeer et al., 2004), (Schallert et al., 2000), (Wydrych, 2010), (Yilmaz et al., 2001). This effect can cause increase of non-uniformity of the solid phase concentration behind the elbow and, in a consequence, worsen of the particle separation by the four-path separator.



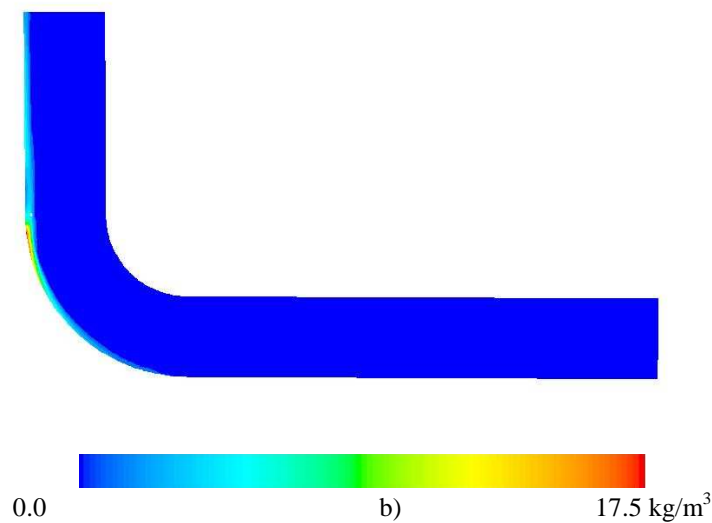


Fig. 5. Distributions of concentration in vertical section obtained with methods a) - EE b) - EL, and c) - ELpl

Analysis of the particle motion trajectories was used for coal dust concentration in the chosen sections. The results of calculations of concentration of the particles delivered to the system from the inlets were presented for all diameters of particle for the inlet velocity 30m/s. Fig.5 shows the results obtained with the EE method – a), the EL method – b) and the ELpl method – c). Method EE gives the results as a volume fraction but for both other unit is $[\text{kg}/\text{m}^3]$

From analysis of particle concentration distribution it appears that a change of the flow direction influences formation of big non-uniformities in rectilinear intervals after the elbows. The centrifugal force causes that thick dust fractions are rejected to the external surfaces of the arcs, and next they move as “the cords” of particles (Akilli et al., 2001), (Hidayat et al., 2005). This effect is undesirable because of segregation of particles, it also causes excessive wear of surfaces of the installation elements in some areas (Abrahamson et al., 2002). From comparison of the results obtained with different methods it appears that the EL and ELpl models shows greater particle concentration at the less area than the EE model. This difference is a result of including collisions between the dust particles of all the phases into the EE model. In the EL and ELpl models it is neglected.

COMPARATIVE ANALYSIS OF THE SIMULATION AND EXPERIMENTAL RESULTS

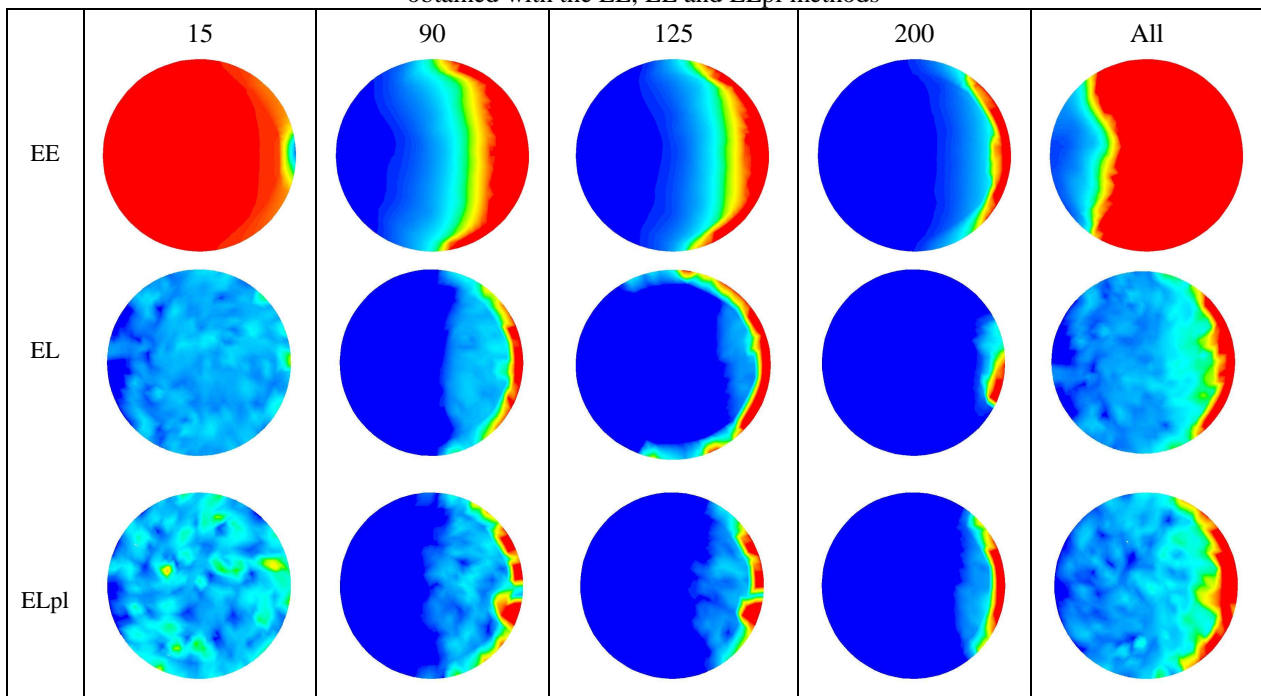
The calculations performed with the Euler-Lagrange (EL, ELpl) and Euler-Euler (EE) methods allowed to determine distributions of the disintegrated phase in the outlet section after the tested elbow. In both methods, the uniform distribution of velocity distribution 30m/s was assumed for the inlet section. The assumed dust mass flow rate was calculated from global rate for inlet section 12.55kg/s and particle concentrations for each phases. In the EL and ELpl methods, the inlet section including 4824 points of particles the trajectories of 19296 particles started. The particles starting their movement in the tested system passed through the elbow area and next they reached the outlet section located just before the four-path separator. In the EE method, an uniform distribution of particle volume fraction at the level 0.9654% was assumed at the inlet section. The results of calculations of the solid phase concentration were recalculated into the units of the mass stream $\text{g}/(\text{cm}^2 \cdot \text{s})$.

Table 1 contains distributions of dust particles 15, 90, 125 and 200 μm in diameters at the outlet after the elbow obtained with the EE, EL and ELpl methods. Maximum results in the

table was truncated to 0.3% for EE method and to $1\text{g}/(\text{cm}^2\cdot\text{s})$ for EE and EEpl methods. On the pictures presented in next part of article inner part of elbow is located on left side of circles.

From the results obtained with the EL and ELpl method for all particle diameters it appears that the particle concentration is increased at the external side of the circle arc as compared with the results obtained with the EE method. The EE method gives more uniform results of calculations of concentration for all the tested particle fractions.

Table 1. Distributions of concentration for particles 15, 90, 125, 200 μm in diameters and for all types of particle obtained with the EE, EL and ELpl methods



Measurements of the distributions of velocity and concentration of dust in the measuring section after the elbow were performed in order to determine the real flow conditions. The measurements were performed in the service conditions (Dobrowolski et al., 2004), (Parys, 2000). The dust samples in the section before the separator were drawn with the device for isokinetic suction. Velocity and concentration distributions are similarly to obtained by other researchers (Barratt et al., 2000).

After comparison particle concentration distribution obtained with experiment and calculation, it appears that particles form big non-uniformities after the elbows. It is especially evident for particles bigger in diameter.

In order to assess qualitative differences between the results obtained with different methods, introduction of a new quantity is suggested, namely the coefficient of variability of concentration distribution of the solid phase V_s . This coefficient was calculated according to the standard deviations of the local value of concentration related to the mean concentration (Wydrych, 2010)

$$V_s = \frac{\frac{1}{n} \sum_{i=1}^n |c_i - \bar{c}|}{\bar{c}} \quad (34)$$

where c_i is the local concentration of the solid phase, \bar{c} is the mean concentration, and n is a size of the calculation points. Table 2 presents values of the variability coefficient for diameters 15, 90, 125, 200 μm and all diameters obtained from calculations according to the EE, EL and ELpl methods.

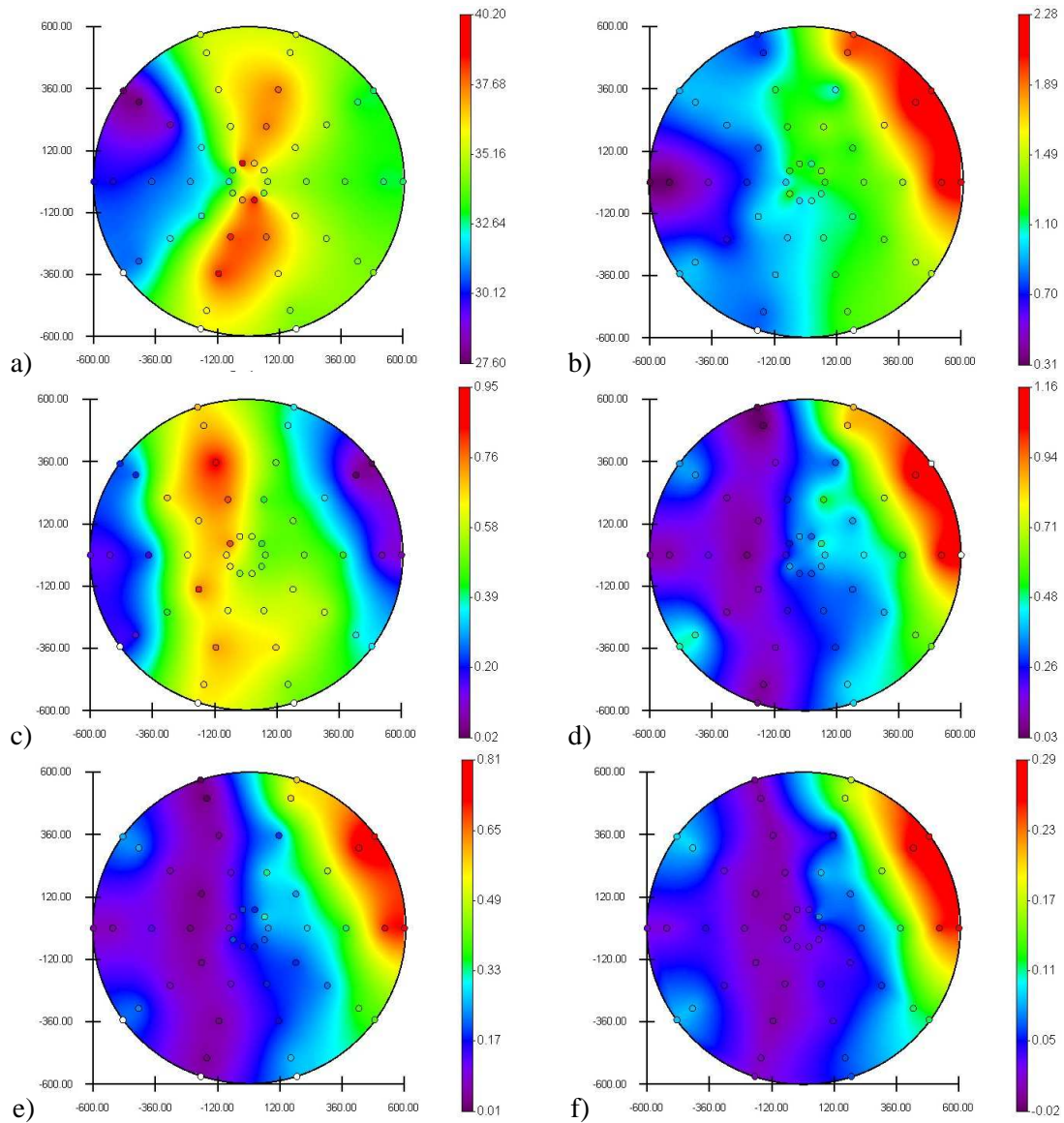


Fig 6. Distributions of a) velocity in [m/s] and concentration in [g/s] for the particles b) all diameters, c) 15, d) 90, e) 125 and f) 200 μ m obtained with experiment

Table 2. Coefficient of variability for distribution of velocity and particle's concentration obtained with experiment, EE, EL and ELpl methods

	Veloc.	200	125	90	15	All
EXP	0.085918	1.178525	0.881735	0.757624	0.481491	0.388447
EE	0.06639	6.36805	5.555911	3.726732	0.04343	3.245496
EL	0.101455	8.030895	5.705094	4.986083	1.073618	3.923967
ELpl	0.083487	7.805772	5.66292	4.880973	0.841747	3.852774

From analysis of characteristics of the variability coefficient it appears that in the case of all the tested particle diameters, the EE, EL and ELpl methods causes more non-uniformities in concentration distributions as compared with experiment (EXP). The particles of big diameters cause increase of non-uniformity, and this is a result of greater inertia.

One of correlation method was used for better recognition obtained distributions. In statistics, Spearman's rank correlation coefficient r_{xy} , is a non-parametric measure of statistical dependence between two variables. It assesses how well the relationship between

two variables can be described using a monotonic function. If there are no repeated data values, a perfect Spearman correlation of +1 or -1 occurs when each of the variables is a perfect monotone function of the other. The Spearman correlation coefficient is defined as the Pearson correlation coefficient between the ranked variables. For a sample of size n , the n raw scores X_i, Y_i are converted to ranks x_i, y_i , and r_{xy} is computed from these:

$$r_{xy} = \frac{\sum_1^n (x_i - \bar{x})(y_i - \bar{y})}{\sqrt{\sum_1^n (x_i - \bar{x})^2 \sum_1^n (y_i - \bar{y})^2}} \quad (35)$$

Table 3 presents possible ranges of correlation from no correlation to perfect correlation. Colors in table mean different level of correlation. This notation was used in next tables, in which are presented comparisons of the results.

Table 3. Scale of r_{xy} values

Positive correlation	Negative correlation	Correlation level
$r_{xy} = 0$	$r_{xy} = 0$	no correlation
$0 < r_{xy} < 0,1$	$-0,1 < r_{xy} < 0$	very weak positive/negative correlation
$0,1 \leq r_{xy} < 0,4$	$-0,4 < r_{xy} \leq -0,1$	weak positive/negative correlation
$0,4 \leq r_{xy} < 0,7$	$-0,7 < r_{xy} \leq -0,4$	moderate correlation
$0,7 \leq r_{xy} < 0,9$	$-0,7 < r_{xy} \leq -0,9$	strong positive/negative correlation
$r_{xy} \geq 0,9$	$r_{xy} \leq -0,9$	very strong positive/negative correlation
$r_{xy} = 1$	$r_{xy} = -1$	perfect positive/negative correlation

Tables 4÷7 present coefficient of correlation for distribution of particle's concentration for experiment, EE, EL and ELpl methods respectively. It is visible that for majority of the methods occurrence negative correlation of particles 15 μ m and bigger particles. This phenomenon is a result of filling volumes by large particles, which cause crowding-out effect for smaller particles. Respectively to works (Akilli et al., 2001), (Bilirgen et al., 2001), (Borsuk et al., 2006), (Fokeer et al., 2004), (Hidayat et al., 2005), (Schallert et al., 2000), (Wydrych, 2010), (Yilmaz et al., 2001) about forming a "cord", authors suggest to introduce a new definition "anti-cord" or "anti-rope". Meaning of this concept is lack of small particles in volumes filled by bigger one. This phenomenon is result of interparticle collisions, which stronger inflow on smaller particles, because their smaller inertia.

Table 4. Coefficient of correlation for distribution of velocity and particle's concentration for result of experiment

	predk	200	125	90	15
All	15.80%	86.61%	92.40%	93.81%	-35.95%
15	46.03%	-73.91%	-68.48%	-65.38%	100.00%
90	-2.69%	95.67%	99.21%	100.00%	
125	-5.68%	97.48%	100.00%		
200	-18.52%	100.00%			

Table 5. Coefficient of correlation for distribution of velocity and particle's concentration for result of EE method

	predk	200	125	90	15
All	-39.99%	99.88%	99.99%	99.98%	99.96%
15	39.44%	99.92%	99.97%	99.90%	100.00%
90	-39.75%	99.74%	99.95%	100.00%	
125	-40.19%	99.92%	100.00%		
200	-40.14%	100.00%			

Table 6. Coefficient of correlation for distribution of velocity and particle's concentration for result of EL method

	predk	200	125	90	15
All	-21.61%	99.88%	99.99%	99.98%	99.96%
15	14.75%	99.92%	99.97%	99.90%	100.00%
90	-8.89%	92.01%	99.95%	100.00%	
125	-11.40%	90.74%	100.00%		
200	-4.67%	100.00%			

Tables 7÷9 present coefficient of mutual correlation for distribution of particle's concentration compared results of experiment with EE, EL and ELpl methods respectively. It is visible that for particles 15µm from experiment occurrence negative correlation for bigger particles from calculations. This effect is similarly to phenomenon described for prior tables.

Comparison last three tables let conclude that Euler-Euler method is the best to calculation of particle distribution in set with elbow. For both other introduction of additional mechanisms cause improvement results for ELpl method. Differences between EE and EL methods are result interparticle collisions included only in Euler-Euler method. Adding this mechanism to Euler-Lagrange methods may improve efficiency of particle's concentration distribution estimation.

Table 7. Coefficient of correlation for distribution of particle's concentration compared results of experiment with EE method

EXP/EE	15	90	125	200	All
15	15.56%	-11.98%	-12.89%	-14.33%	-12.34%
90	-81.62%	78.78%	79.40%	80.31%	79.03%
125	-79.93%	77.15%	77.50%	78.02%	77.33%
200	-66.28%	62.57%	62.92%	63.43%	62.77%
All	-93.44%	93.27%	93.27%	93.30%	93.32%

Table 8. Coefficient of correlation for distribution of particle's concentration compared results of experiment with EL method

EXP/EL	15	90	125	200	All
15	11.16%	-21.57%	-3.88%	-2.76%	-18.61%
90	6.29%	77.47%	58.35%	54.29%	67.85%
125	4.21%	77.80%	59.15%	53.70%	67.02%
200	14.14%	72.05%	57.19%	51.18%	57.90%
All	41.56%	81.32%	64.80%	58.92%	75.10%

Table 9. Coefficient of correlation for distribution of particle's concentration compared results of experiment with ELpl method

EXP/ELpl	15	90	125	200	All
15	15.75%	-21.91%	-14.77%	14.91%	-21.66%
90	28.68%	79.42%	70.45%	63.42%	69.69%
125	25.76%	80.00%	70.19%	62.88%	68.13%
200	23.57%	68.85%	66.74%	60.57%	58.63%
All	14.87%	83.71%	74.36%	67.58%	79.44%

CONCLUSIONS

The performed investigations allow to formulate some important conclusions. From analysis of trajectories it appears that the particles of small diameters move along the paths corresponding to the lines of the gaseous phase current, and the particles of big diameters often move along the paths forming a “cord” – this is a reason of the local increase of concentration.

The results obtained with the EL and ELpl methods for all diameters of particles prove the increased concentration of particles at the external side of the circle arc in relation to the results obtained with the EE method. The EE method gives more uniform results of concentration calculations for all the tested particle fractions. This difference is a result of including collisions between the dust particles in the EE model, omitted in the EL and ELpl models.

The coefficient of variability of concentration distribution of the solid phase V_s was proposed. Comparison of the variability coefficients allows to state that simulation using the Euler- Euler method gives the results closer to the test results.

Coefficient of correlation was used in work for better recognition obtained distributions. Results show that for majority of the methods occurrence negative correlation of particles 15 μ m and bigger particles. This phenomenon is a result of filling volumes by large particles, which cause crowding-out effect for smaller particles. Authors suggest to introduce a new definition “**anti-cord**”.

Comparison reciprocal correlation for distribution of particle's concentration from experiment with EE, EL and ELpl methods shows that for particles 15 μ m from experiment occurrence negative correlation for bigger particles from calculations.

Researches let conclude that Euler-Euler method is the best to calculation of particle distribution in set with elbow. Differences between EE and EL methods are result interparticle collisions included only in Euler-Euler method. Adding this mechanism to Euler-Lagrange methods may improve efficiency of particle's concentration distribution estimation.

The observed quantitative differences can result from the assumed simplifications and three-dimensionality of the flow in the tested system. It limits the applicability range of the methods used for the measurements of dust velocity and concentration.

In such situations, the results obtained according to the Euler-Lagrange model are incorrect, and the error is a result of application of an incorrect method of calculations. In the case of volume fractions of solid particles in gas exceeding 12%, the Euler-Euler method (so-called Euler methods) seems to be more useful, and this method can be recommended to the further investigations.

REFERENCES

- Abrahamson J., Jones R., Lau A., Reveley S. (2002): *Influence of entry duct bends on the performance of return-flow cyclone dust collectors*, Powder Technology 123, 126–137
- Akilli H., Levy E.K., Sahin B. (2001): *Gas–solid flow behavior in a horizontal pipe after a 90° vertical-to-horizontal elbow*, Powder Technology, 116, 43–52

- Albion K., Briens L., Briens C., Berruti F., Book G. (2007): *Flow regime determination in upward inclined pneumatic transport of particulates using non-intrusive acoustic probes*, Chemical Engineering and Processing 46, 520–531
- Barratt I.R., Yan Y., Byrne B., Bradley M.S.A. (2000): *Mass flow measurement of pneumatically conveyed solids using radiometric sensors*, Flow Measurement and Instrumentation 11, 223–235
- Bilirgen H., Levy E.K. (2001): *Mixing and dispersion of particle ropes in lean phase pneumatic conveying*, Powder Technology, 119, 134–152
- Borsuk G., Dobrowolski B., Wydrych J. (2006): *Gas - solids mixture flow through a two-bend system*, Chemical and Process Engineering, vol. 27, nr 3/1, 645-656
- Dobrowolski B., Pospolita J., Wydrych J. (2004): *Próba poprawy warunków przepływowych przed rozdzielaczem czterodrogowym w układzie pyłowym kotła BP-1150*, Inżynieria chemiczna i procesowa, vol. 25 z. 4, 2105-2112
- Dobrowolski B., Wydrych J. (2006): *Evaluation of numerical models for prediction of areas subjected to erosion wear*, Int. J. of Applied Mechanics and Engineering, vol.11, No.4, 735-749
- Dodds D., Naser J., Staples J., Black C., Marshall L., Nightingale V. (2011): *Experimental and numerical study of the pulverised-fuel distribution in the mill-duct system of the Loy Yang B lignite fuelled power station*, Powder Technology 207, 257–269
- El-Behery S.M., Hamed M.H., El-Kadi M.A., Ibrahim K.A. (2009): *CFD prediction of air–solid flow in 180° curved duct*, Powder Technology, 191, 130–142
- Fokeer S., Kingmana S., Lowndes I., Reynolds A. (2004): *Characterisation of the cross sectional particle concentration distribution in horizontal dilute flow conveying—a review*, Chemical Engineering and Processing, 43, 677–691
- Hidayat M., Rasmuson A. (2005): *Some aspects on gas–solid flow in a U-bend: Numerical investigation*, Powder Technology, 153, 1– 12
- Jaworski A.J., Dyakowski T. (2002): *Investigations of flow instabilities within the dense pneumatic conveying system*, Powder Technology, 125, 279– 291
- Kosinski P., Hoffmann A.C. (2010): *An extension of the hard-sphere particle–particle collision model to study agglomeration*, Chemical Engineering Science, 65, 3231–3239
- Kuan B., Yang W., Schwarz M.P. (2007): *Dilute gas–solid two-phase flows in a curved 90° duct bend: CFD simulation with experimental validation*, Chemical Engineering Science, 62, 2068–2088
- Lain S., Sommerfeld M. (2012): *Numerical calculation of pneumatic conveying in horizontal channels and pipes: Detailed analysis of conveying behavior*, International Journal of Multiphase Flow 39, 105–120
- Levy A., Mason D.J. (1998): *The effect of a band on the particle cross-section concentration and segregation in pneumatic conveying systems*, Powder Technology, 98, 95-103
- Lu Y., Glass D.H., Easson W.J. (2009): *An investigation of particle behavior in gas–solid horizontal pipe flow by an extended LDA technique*, Fuel, 88, 2520–2531
- Miller R.M., Singh J.P., Morris J.F. (2009): *Suspension flow modeling for general geometries*, Chemical Engineering Science 64, 4597 -- 4610

- Parys R. (2000): *Pomiary rozptyłu mieszanki w rozdzielaczu czterodrogowym w instalacji pyłowej młyna 4MW3 w Elektrowni Opole*, Praca wykonana przez firmę Introl na zlecenie Elektrowni Opole, Opole
- Rajniak P., Dhanasekharan K., Sinka C., MacPhail N., Chern R. (2008): *Modeling and measurement of granule attrition during pneumatic conveying in a laboratory scale system*, Powder Technology, 185, 202–210
- Schallert R., Levy E. (2000): *Effect of a combination of two elbows on particle roping in pneumatic conveying*, Powder Technology 107, 226–233
- Spedding P.L., Benard E. (2007): *Gas-liquid two phase flow through a vertical 90° elbow bend*, Experimental Thermal and Fluid Science, 31, 761–769
- Triesch O., Bohnet M. (2001): *Measurement and CFD prediction of velocity and concentration profiles in a decelerated gas-solids flow*, Powder Technology, 115, 101–113
- Wang J., Shirazi S.A. (2001): *A CFD based correlation for mass transfer coefficient in elbows*, International Journal of Heat and Mass Transfer, 44, 1817-1822
- Woods J.A., Thorpe R.B., Johnson S.E. (2008): *Horizontal pneumatic conveying from a fluidized bed*, Chemical Engineering Science, 63, 1741 – 1760
- Wydrych J. (2007): *Computational and experimental analysis of gas-particle flow in furnace power boiler installations with respect to erosion phenomena*, Journal of theoretical and applied mechanics, vol.45, No.3, 513-538
- Wydrych J., Szmolke N. (2010): *Reciprocal correlation in fluid flows*, Int. Conference of Modeling and Simulation – Virtual Forum, Italy , Napoli, 12-26.07.2010
- Wydrych J. (2010): *Comparative analysis of the methods of simulation of flow in boiler dust systems*, Chemical and Process Engineering, vol. 31, nr 4, 603-623
- Wydrych J. (2011): *Diagnozowanie zużycia erozyjnego instalacji transportu pneumatycznego w przemyśle cementowym*, Nauka i praktyka - staże zawodowe w przedsiębiorstwach. Edycja II Opole, Ofic.Wydaw.PO, 73-81,
- Yilmaz A., Levy E.K. (2001): *Formation and dispersion of ropes in pneumatic conveying*, Powder Technology 114, 168–185